

---

# JOURNAL OF THE AMERICAN CHEMICAL SOCIETY

---

## A Self-Folding Metallocavitand

Ulrich Lücking, Jian Chen, Dmitry M. Rudkevich,<sup>\*,†</sup> and Julius Rebek, Jr.<sup>\*</sup>

Contribution from The Skaggs Institute for Chemical Biology and The Department of Chemistry,  
The Scripps Research Institute, MB-26, 10550 North Torrey Pines Road, La Jolla, California 92037

Received June 18, 2001

**Abstract:** The synthesis and characterization of novel metallocavitand **6** are described. This is a covalent hybrid of a deepened, self-folding cavity and a Zn–phenanthroline fragment. Host **6** features a large molecular cavity of  $\sim 8 \times 10 \text{ \AA}$  dimensions, and the metal binding site is directed in toward the cavity. Binding abilities of the metallocavitand in solution was demonstrated for quinuclidine **11** and Dabco **12** using UV–vis and  $^1\text{H}$  NMR spectroscopy. Intramolecular hydrogen bonds at the upper rims of cavitand **6** resist the unfolding of the inner cavities and thereby increase the energetic barrier to guest exchange. The exchange is slow on the NMR time scale (at ambient temperatures,  $\text{CD}_2\text{Cl}_2$ ), and kinetically stable complexes result. Both the polyaromatic cavity and metallosite participate simultaneously in the binding event. Zinc-containing deep cavities may be attractive as catalytic chambers for hydrolysis and esterification.

### Introduction

Functionalization of concave surfaces with metal centers is one of the pursuits of molecular recognition and holds promise for enzyme mimicry.<sup>1</sup> Receptors incorporating a metallosite–metalloreceptors—have been widely used for recognition of anions and neutral organic molecules;<sup>2</sup> molecular clefts and concave reagents containing Lewis acids are numerous, but there are only a few examples of metal binding sites combined with synthetic molecular cavities that more or less completely surround their guests (Figure 1).<sup>3</sup> In phosphonite-bridged metallocavitands **1**, four Au(I), Cu(I), and Ag(I) binding centers

operate, even cooperate, with the macrocyclic cavity to sequester alkylamines and halide anions.<sup>4</sup> For example, in the tetrasilver-(I) cavitand **1**, an encapsulated  $\text{Cl}^-$  anion behaved as a nucleophile to alkyl iodides to give alkyl chlorides. Tris(imidazole)-Zn-calix[6]arene receptor **2** effectively binds polar organic guests—alkylamines, alcohols, nitriles, and so forth,—both in solution and in the solid state, through metal–ligand coordination and encapsulation within the hydrophobic calixarene cavity.<sup>5</sup> Calix[4]arenes **3**<sup>6</sup> and **4**,<sup>7</sup> possessing Pd(II) or Zn–porphyrin binding sites, respectively, trap a number of pyridines within their cavities. In these cases, the substrate binding occurs primarily via metal $\cdots\text{N}$  interactions, but the

<sup>†</sup> Present address: Department of Chemistry and Biochemistry, The University of Texas at Arlington, Box 19065, Arlington, TX 76019.

(1) Murakami, Y.; Kikuchi, J.; Hisaeda, Y.; Hayashida, O. *Chem. Rev.* **1996**, *96*, 721–758.

(2) Metalloreceptors and metalloclefts: Rudkevich, D. M.; Huck, W. T. S.; van Veggel, F. C. J. M.; Reinhoudt, D. N. In *Transition Metals in Supramolecular Chemistry*; Fabbrizzi, L., Poggi, A., Eds.; Kluwer Academic Publishers: Dordrecht, Boston, London, 1994; p 329–349. Concave reagents: (a) Lüning, U. *Top. Curr. Chem.* **1995**, *175*, 57–99.

(3) Rudkevich, D. M.; Rebek, J., Jr. *Eur. J. Org. Chem.* **1999**, 1991–2005. For examples of calixarenes in transition metal chemistry, see: Weiser, C.; Dieleman, C. B.; Matt, D. *Coord. Chem. Rev.* **1997**, *165*, 93–161.

(4) (a) Xu, W.; Rourke, J. P.; Vittal, J. J.; Puddephatt, R. J. *Inorg. Chem.* **1995**, *34*, 323–329. (b) Xu, W.; Vittal, J. J.; Puddephatt, R. J. *J. Am. Chem. Soc.* **1995**, *117*, 8362–8371.

(5) Seneque, O.; Rager, M.-N.; Giorgi, M.; Reinaud, O. *J. Am. Chem. Soc.* **2000**, *122*, 6183–6189. See also: Wieser-Jeunesse, C.; Matt, D.; De Cian, A. *Angew. Chem., Int. Ed.* **1998**, *37*, 2861–2864. See also: Fan, M.; Zhang, H.; Lattman, M. *Chem. Commun.* **1998**, 99–100.

(6) Loeb, S. J.; Cameron, B. R. In *Calixarene Molecules for Separations*; Lumetta, G., Rogers, R. D., Gopalan, A. S., Eds.; ACS Symposium Series; Washington, DC, 2000; pp 283–295.

(7) Rudkevich, D. M.; Verboom, W.; Reinhoudt, D. N. *J. Org. Chem.* **1995**, *60*, 6585–6587.

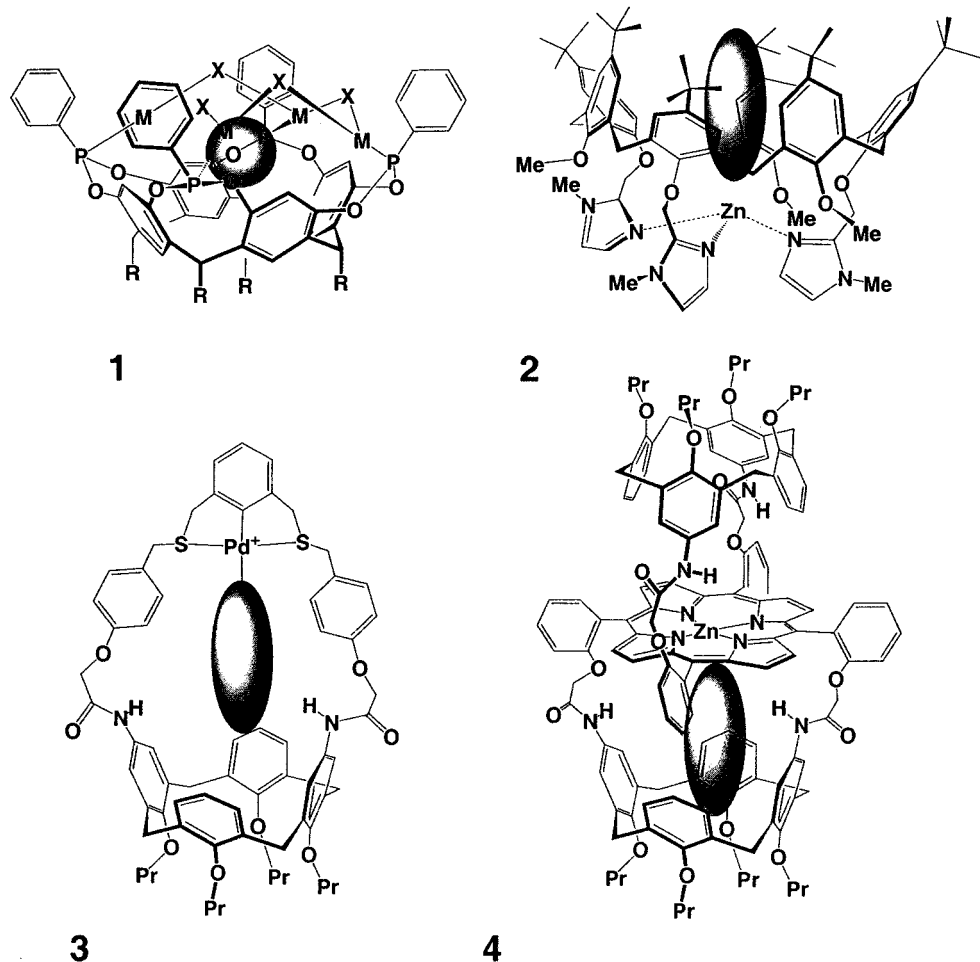


Figure 1. Metal-containing molecular cavities 1–4.<sup>4–7</sup>

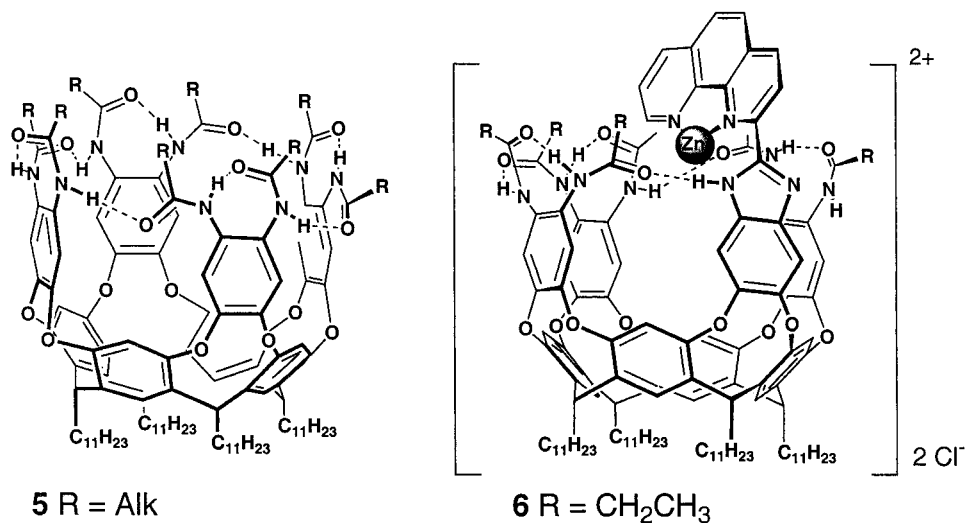


Figure 2. Self-folding cavitand 5<sup>8</sup> (only one cycloenantiomer is depicted) and self-folding metallocavitand 6.

calixarene cavity incidentally participates in shielding the guest from the bulk solution.

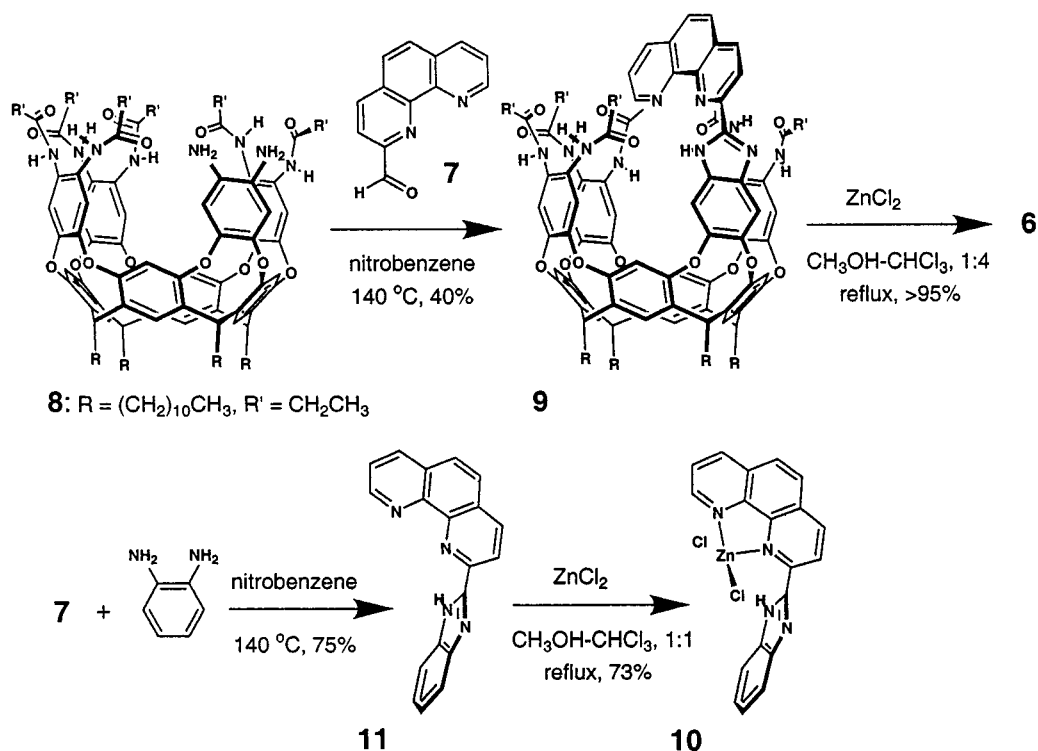
In all of these examples, the molecular cavity's dimensions are not sizable ( $\leq 4$  Å). Accordingly, their ability to surround the guests is marginal; instead, the overall binding in metallocavitands 1–4 is largely due to direct contacts with the metals.

We recently introduced (and named) deep, self-folding cavitand hosts 5 (Figure 2). In these structures, the cyclic array of eight cooperative hydrogen bonds provided by the secondary

amides maintains the four aromatic walls in a vase-like conformation.<sup>8</sup> The seam of hydrogen bonds resists the unfolding of the vase required for guest exchange. The kinetic stabilities of the host–guest complexes are high and feature slow exchange in solution on the NMR time scale. We report

(8) (a) Rudkevich, D. M.; Hilmersson, G.; Rebek, J., Jr. *J. Am. Chem. Soc.* **1998**, *120*, 12216–12225. (b) Ma, S.; Rudkevich, D. M.; Rebek, J., Jr., *Angew. Chem. Int. Ed.* **1999**, *38*, 2600–2602. (c) Shivanyuk, A.; Rissanen, K.; Körner, S. K.; Rudkevich, D. M.; Rebek, J., Jr. *Helv. Chim. Acta* **2000**, *83*, 1778–1790.

Scheme 1



here the synthesis and host–guest properties of a self-folding, metal-containing cavitaand **6**, a *metallocavitand*. The structure of **6** combines a deepened (8 × 10 Å) self-folding cavity and a Lewis acidic metal center presented to its interior (Figure 2). The arrangement offers an additional binding site and a well-positioned, potentially catalytic functionality.<sup>9</sup>

## Results and Discussion

**Synthesis (Scheme 1).** Condensation of 1,10-phenanthroline-2-carbaldehyde **7**<sup>10</sup> with previously reported diamine cavitaand **8**<sup>11</sup> in hot nitrobenzene as solvent and oxidant gave metal-free cavitaand **9** in 40% yield. Compound **9** was quantitatively converted to metallocavitand **6** with ZnCl<sub>2</sub> in boiling CHCl<sub>3</sub>/MeOH, (4:1).<sup>12</sup> The simpler Zn–phenanthroline complex **10** was likewise prepared for comparison purposes.

(9) Several other cavities functionalized with metal centers are known. Cyclodextrins: (a) Kuroda, Y.; Hiroshige, T.; Sera, T.; Shirowai, Y.; Tanaka, H.; Ogoshi, H. *J. Am. Chem. Soc.* **1989**, *111*, 1912–1913. (b) Kuroda, Y.; Ito, M.; Sera, T.; Ogoshi, H. *J. Am. Chem. Soc.* **1993**, *115*, 7003–7004. (c) Breslow, R.; Dong, S. D. *Chem. Rev.* **1998**, *98*, 1997–2011. (d) Engeldinger, E.; Armpach, D.; Matt, D. *Angew. Chem., Int. Ed.* **2001**, *40*, 2526–2529. (e) Armpach, D.; Matt, D.; Kyritsakas, N. *Polyhedron* **2001**, *20*, 663–668. Steroid-capped porphyrins: (f) Bonar-Law, R. P.; Sanders, J. K. M. *J. Am. Chem. Soc.* **1995**, *117*, 259–271; Bonar-Law, R. P.; Sanders, J. K. M. *J. Chem. Soc., Perkin Trans. 1* **1995**, 3085–3096. Cavitaand-porphyrins: (g) Starnes, S. D.; Rudkevich, D. M.; Rebek, J., Jr. *J. Am. Chem. Soc.* **2001**, *123*, 4659–4669. (h) Calix[4]salenes: Rudkevich, D. M.; Verboom, W.; Reinhoudt, D. N. *J. Org. Chem.* **1994**, *59*, 3683–3686.

(10) Weijnen, J. G.; Koudijs, A.; Engbersen, J. F. J. *J. Chem. Soc., Perkin Trans. 2* **1991**, 1121–1126.

(11) Lücking, U.; Tucci, F. C.; Rudkevich, D. M.; Rebek, J., Jr. *J. Am. Chem. Soc.* **2000**, *122*, 8880–8889.

(12) A structural analogue of **9** with longer alkyl chains (R = (CH<sub>2</sub>)<sub>6</sub>CH<sub>3</sub>) was also prepared: <sup>1</sup>H NMR (CD<sub>2</sub>Cl<sub>2</sub>, 295 K): 12.82 (s, 1 H), 10.02 (s, 1 H), 9.76 (s, 1 H), 9.56 (s, 1H), 9.10 (d, J = 2.8 Hz, 1 H), 8.97 (s, 1 H), 8.95 (s, 1 H), 8.77 (s, 1 H), 8.40–8.20 (m, 3 H), 7.95–7.60 (m, 8 H), 7.55–7.10 (m, 12 H), 5.80–5.62 (4 × t, J = 8 Hz, 4 H), 2.80–0.50 (m, 182 H); MALDI-TOF *m/z* 2470 ([M + H]<sup>+</sup>, calcd for C<sub>157</sub>H<sub>216</sub>N<sub>10</sub>O<sub>14</sub> = 2469).

**Spectroscopic Features.** Extensive FTIR and NMR spectroscopic studies, single-crystal X-ray analysis and molecular modeling,<sup>8,11</sup> have established that the upper rim of self-folding cavitaands and their derivatives feature a seam of intramolecular hydrogen bonds. The <sup>1</sup>H NMR spectra of **6** and **9** are sharp in deuterated, chlorinated solvents at room temperature (Figure 3), and modeling<sup>13</sup> suggests that its amides are stitched in a seam of five intramolecular hydrogen bonds within a vase-like structure. A unique hydrogen bond is formed between the benzimidazole NH and its neighboring amide C=O oxygen. All amide NH resonances are singlets for **6** and **9** and they are situated downfield of 8 ppm in CD<sub>2</sub>Cl<sub>2</sub> as expected for strong hydrogen bonding; the benzimidazole NH is seen at ~12 ppm. The head-to-tail seam results in two cycloenantiomers,<sup>14</sup> with clockwise and counterclockwise orientation of the HN–CO bonds, and the interconversion between those is apparently slow on the NMR time scale. The <sup>1</sup>H NMR spectra indicated that the molecules **6** and **9** have no mirror plane, and all NH protons are magnetically nonequivalent (Figure 3). This has also been observed for other benzimidazole-containing self-folding cavitaands.<sup>11</sup> Since the benzimidazole NH proton is involved, the seam's cycloracemization would require the tautomerization of this heterocycle.

The <sup>1</sup>H NMR spectra also showed the spectroscopic features of the vase conformation of the cavities in **6** and **9** (CD<sub>2</sub>Cl<sub>2</sub>, 295 K), with the characteristic<sup>8,11</sup> methine CH signals at ~6 ppm.

(13) MacroModel 7.0; Amber\* Force Field; Mohamadi, F.; Richards, N. G.; Guida, W. C.; Liskamp, R.; Lipton, M.; Caufield, C.; Chang, G.; Hendrickson, T.; Still, W. C. *J. Comput. Chem.* **1990**, *11*, 440–467.

(14) Cycloenantiomerism: (a) Prelog, V.; Gerlach, H. *Helv. Chim. Acta* **1964**, *47*, 2288–2294. (b) Goodman, M.; Chorev, M. *Acc. Chem. Res.* **1979**, *12*, 1–7. (c) Yamamoto, C.; Okamoto, Y.; Schmidt, T.; Jäger, R.; Vögtle, V. *J. Am. Chem. Soc.* **1997**, *119*, 10547–10548. In agreement with the Prelog's terminology, enantiomers **5** possess the clockwise and counterclockwise "directionality" of the eight secondary amide "building blocks" in an otherwise identical "distribution pattern", or the sequence of connectivity.

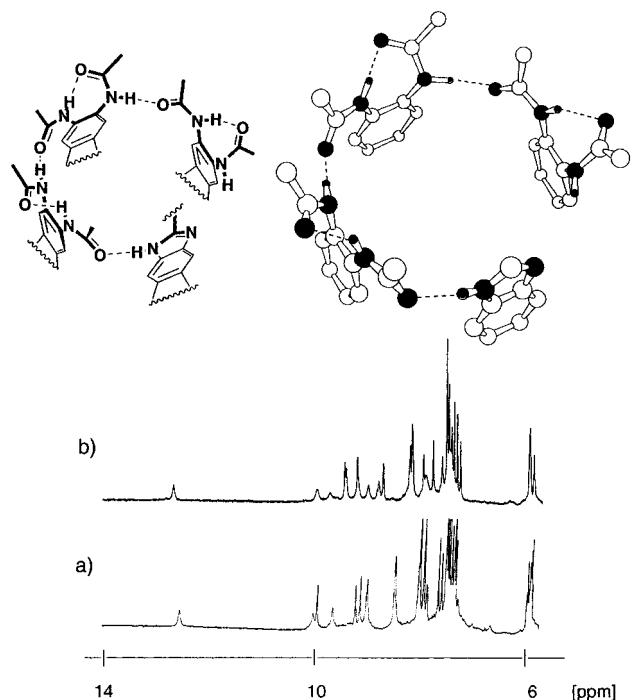


**Figure 3.** (Top) Hydrogen bonding in cavitands **6** and **9** (part of the structure). (Bottom) Portions of the <sup>1</sup>H NMR spectra of (600 MHz, CD<sub>2</sub>Cl<sub>2</sub>, 295 K) of: (a) **9** and (b) **6**. In the downfield region, all nonequivalent NH singlets and four phenanthroline signals are seen at 8–13 ppm. The methine CH triplets are situated at 6–5.5 ppm. See also Experimental Section.

**Host–Guest Properties.** Complexation of guest species by metallocavitand **6** exhibits a number of unique features. The Zn(II)–phenanthroline complex **6** is diamagnetic and stable to oxidation. Due to the d<sup>10</sup> electronic configuration of zinc, a variety of coordination polyhedra (e.g., 4, 5, or 6) is possible; the complexes often show deviations from regular geometries.<sup>15</sup> A number of Zn(II)–phenanthroline complexes have already been employed for ester, amide, and phosphate hydrolysis.<sup>10,16</sup> According to molecular modeling,<sup>13</sup> the internal cavity in metallocavitand **6** is ~8–9 Å deep, from the bottom to the metal center, and 10 Å wide. At first glance, the phenanthroline fragment might freely rotate with respect to the cavity, but the alkyl groups of the amides must provide some steric clashes. Instead, it is likely that the phenanthroline adopts one of two ground-state conformations, endo or exo with respect to the cavity. As with other self-folding cavitands,<sup>8</sup> adamantyl-containing guest molecules were seen entrapped within the cavities of **6** and **9**. Due to the ring currents of the cavity's aromatic walls,<sup>8</sup> the <sup>1</sup>H NMR signals of the accommodated guests were seen upfield 0 ppm at room temperatures; integration clearly indicates the 1:1 stoichiometry for the complexes.

Next, tertiary amines such as quinuclidine **11** and 1,4-diazabicyclo[2.2.2]octane (Dabco) **12** were studied as their semispherical aliphatic skeleton (~4 Å diameter) showed a snug fit within the cavitand interior and the nitrogen atom is expected to strongly coordinate with the Zn–phenanthroline fragment (Figure 4). Both metallocavitand **6** and even its metal-free analogue **9** showed kinetically stable complexes with

(15) Müller-Hartmann, A.; Vahrenkamp, H. *Eur. J. Inorg. Chem.* **2000**, 2355–2361 and references therein. See also: (a) Löffler, F.; Lünig, U.; Gohar, G. *New J. Chem.* **2000**, *24*, 935–938. (b) Mather, D. W.; Goodwin, H. A. *Aust. J. Chem.* **1975**, *28*, 505–511.

(16) (a) Sigman, D. S.; Wahl, G. M.; Creighton, D. J. *Biochemistry* **1972**, *11*, 2236–2242. (b) Creighton, D. J.; Hajdu, J.; Sigman, D. S. *J. Am. Chem. Soc.* **1976**, *98*, 4619–4625.

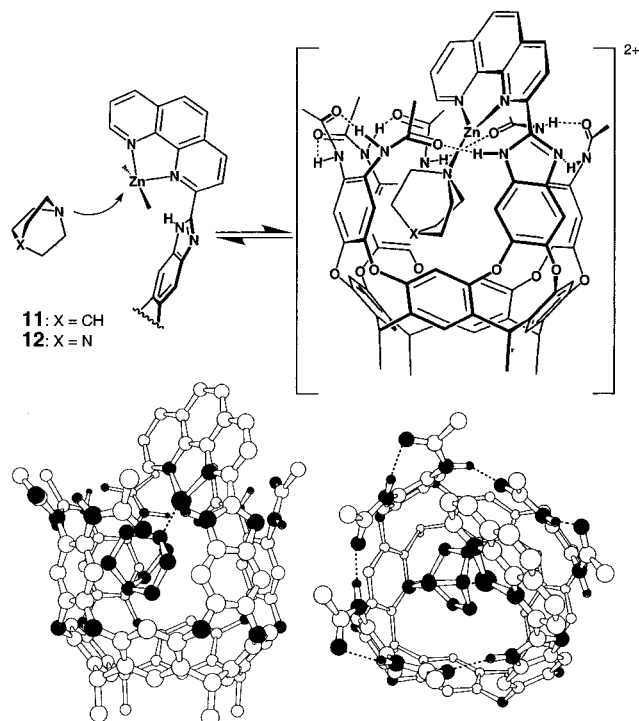


**Figure 4.** (Top) Guests **11** and **12** and their complexes with metallocavitand **6**. (Bottom) Energy-minimized<sup>13</sup> structures of the Dabco complex **6·12**. Alkyl chains and CH bonds were omitted for viewing clarity. The Zn–phenanthroline geometrical parameters were adopted from literature.<sup>15a</sup> Only one cycloenantiomer is depicted.

**11** and **12**: slow exchange between the free and complexed guests was observed on the NMR time scale at room temperature. The bound guest signals were seen upfield of 0 ppm. Moreover, *no tumbling* of guests **11** and **12** inside either cavity was detected.

For the quinuclidine complex **9·11**, two broad signals (6:1 ratio) of the skeleton's CH protons were clearly seen at –1.44 and –1.97 ppm, respectively. The corresponding chemical shifts of uncomplexed **11** in CD<sub>2</sub>Cl<sub>2</sub> are 2.8 and 1.7 ppm, respectively. The methine CH proton of **11** was seen the most upfield-shifted indicating that it is oriented toward the bottom of the cavity. As a result, the CH protons of the upper part are not as shielded by the cavity's walls, and they do not appear in the upfield window. For the Dabco complex **9·12**, two broad singlets (1:1 ratio) of the skeleton CH protons were seen at 0.64 and –0.07 ppm. The corresponding, single (!) chemical shift of uncomplexed Dabco **12** in CD<sub>2</sub>Cl<sub>2</sub> is 2.7 ppm.

For metallocavities **6·11** and **6·12**, the CH<sub>2</sub> methylene protons of entrapped guests were seen as *doubled sets* (Figure 5), with the shifts values comparable to the metal-free complexes **9·11** and **9·12**.

Upon addition of guests **11** and **12**, the UV–vis maxima at 370 nm of the solution of metallocavitand **6** in CD<sub>2</sub>Cl<sub>2</sub> is shifted ~30 nm bathochromic; similar behavior was observed upon titration of model Zn complex **10**.<sup>17</sup> This clearly indicates that the Zn···N interactions between the metallosite and the guest take place. This was further confirmed by a competition experiment. Equimolar quantities of cavitands **6** and **9** and Dabco **12** were mixed in CD<sub>2</sub>Cl<sub>2</sub> solution at 295 K, and the

(17) Only a 1:1 stoichiometry was detected for the complex **6·12** by <sup>1</sup>H NMR spectroscopy (CD<sub>2</sub>Cl<sub>2</sub>, 295 K), and modeling suggested that significant steric and electronic repulsions would occur with other stoichiometries. Under these conditions however, a number of different stoichiometries was detected for the complexes of model Zn–phenanthroline **10** and Dabco **12**. See also ref 15.

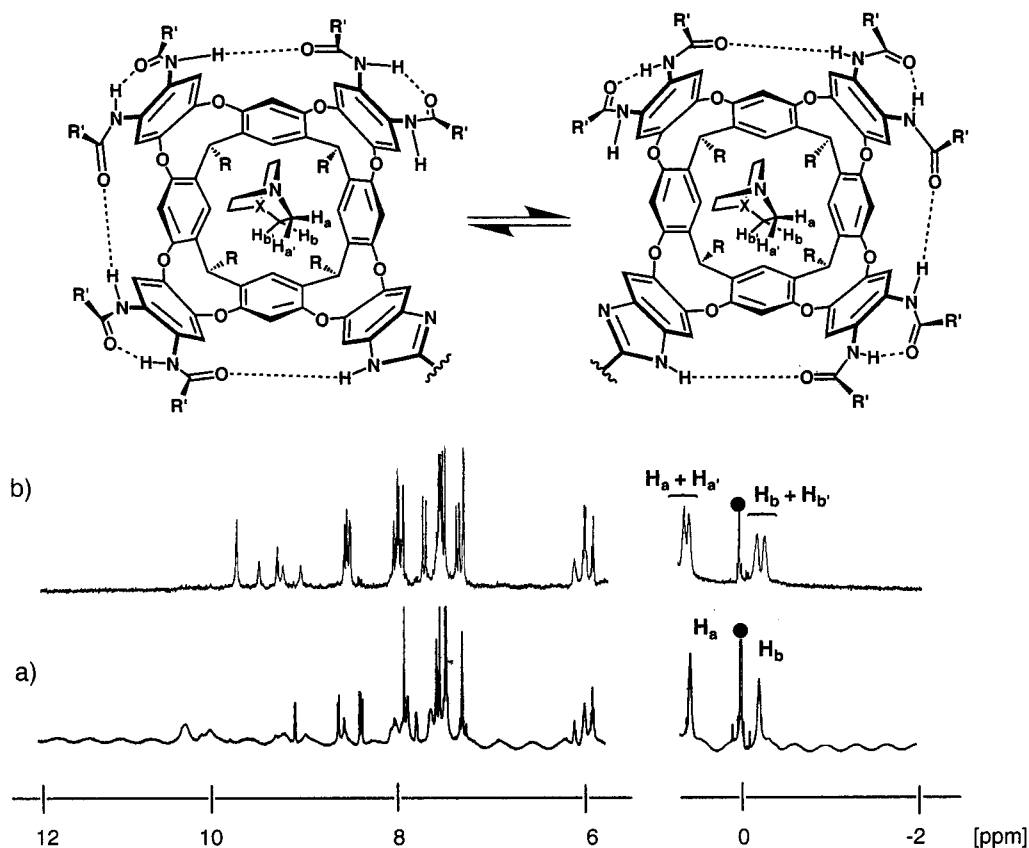


**Figure 5.** (Top) Schematic representation of cycloenantiomerism in metallocavitand **6** and its complexes with guests **11** and **12**. (Bottom) portions of the  $^1\text{H}$  NMR spectra of (600 MHz,  $\text{CD}_2\text{Cl}_2$ , 295 K) of complexes: (a) **9**·**12** and (b) **6**·**12**. The guest's diastereotopic protons are marked.

upfield  $^1\text{H}$  NMR signals of the complexed Dabco were integrated. Complex **6**·**12** formed predominantly ( $\geq 5:1$ ) which indicates that it is at least  $1 \text{ kcal mol}^{-1}$  more stable than complex **9**·**12**. Accordingly, in metallocavitand **6** bidentate 1:1 binding occurred, with the guest's skeleton entrapped within the inner cavity and the amine nitrogen atom complexed to the Zn–phenanthroline site (Figure 4).

The  $^1\text{H}$  NMR spectra of the complexes **6**·**11** and **6**·**12** are sharp (295 K); all amide N–H signals were seen separately, indicating that the interconversion between the cycloenantiomers within the complex is slow. This results in the chiral inner environment of the cavity, and the enantiotopic  $\text{CH}_a\text{H}_{a'}$  and  $\text{CH}_b\text{H}_{b'}$  methylene protons of **11** and **12** become respectively diastereotopic. Two sets of the corresponding signals were clearly seen in the  $^1\text{H}$  NMR spectra, and their assignment was further confirmed by COSY experiments. At the same time, while the spectra of the metal-free complexes **9**·**11** and **9**·**12** are also sharp (295 K), the corresponding amide N–H signals significantly broaden, indicating that some dynamic process, probably the interconversion of cycloenantiomers, is intermediate in rate. The inner cavity is not chiral on the NMR time scale, and the  $\text{CH}_a\text{H}_{a'}$  and  $\text{CH}_b\text{H}_{b'}$  methylene protons of **11** and **12** are respectively equivalent (Figure 5). In other words, the DABCO guest catalyzes the racemization of the metal-free cavitaand.

In summary, self-folding metallocontainers are introduced for selective molecular recognition with an eye toward applications in catalysis. Guest complexation of appropriate amines is shown to take place within the inner cavity *with* metal–ligand participation. The use of zinc-containing cavities as catalytic chambers for hydrolysis and esterification beckons, and the preparation of water-soluble and polymer-supported versions of these next-generation synthetic hosts is underway.<sup>18,19</sup>

## Experimental Section

**General.** Melting points were determined on a Thomas-Hoover capillary melting point apparatus and are uncorrected.  $^1\text{H}$  NMR and  $^{13}\text{C}$  NMR spectra were recorded on Bruker DRX-600 spectrometer. Chemical shifts were measured relative to residual nondeuterated solvent resonances. FTIR spectra were recorded on a Perkin-Elmer Paragon 1000 PC FT-IR spectrometer. UV–vis spectra were recorded on a Perkin-Elmer UV/Vis Lambda 12 spectrometer. High-resolution matrix-assisted laser desorption/ionization mass spectrometry (HR MALDI FTMS) experiments were performed on a IonSpec HiResMALDI Fourier transform mass spectrometer. Electrospray ionization mass spectra (ESI MS) were recorded on an API III Perkin-Elmer SCIEX triple quadrupole mass spectrometer. Mass spectral data with lower resolution were obtained for compounds with molecular weight  $\geq 2000$ .<sup>20</sup> Column chromatography was performed with Silica Gel 60 (EM Science or Bodman, 230–400 mesh). All experiments with moisture- or air-sensitive compounds were performed in anhydrous solvents under a nitrogen or argon atmosphere. Molecular modeling was performed using the Amber\* force field in MacroModel 7.0.<sup>13</sup>

**Cavitand 9.** A solution of phenanthrolinecarbaldehyde<sup>10</sup> **7** (9.4 mg, 44.6  $\mu\text{mol}$ ) in nitrobenzene (2 mL) was added to the crude diamine<sup>11</sup> **8** (74 mg, 40  $\mu\text{mol}$ ), the resulting solution was evacuated, and the reaction flask was filled with  $\text{N}_2$ . The reaction mixture was stirred at 140  $^\circ\text{C}$  for 22 h. The solvent was removed under vacuum, and the residue was purified by column chromatography ( $\text{CH}_2\text{Cl}_2$ –MeOH,

(18) For the synthesis of water-soluble self-folding cavitaands, see: Haino, T.; Rudkevich, D. M.; Shivanyuk, A.; Rissanen, K.; Rebek, J., Jr. *Chem. Eur. J.* **2000**, *6*, 3797–3805.

(19) Preliminary results on polymer-supported self-folding cavitaands: Rafai Far, A.; Rudkevich, D. M.; Haino, T.; Rebek, J., Jr. *Org. Lett.* **2000**, *2*, 3465–3468.

(20) For details, see: (a) Rose, M. E.; Johnstone, R. A. W. *Mass Spectrometry for Chemists and Biochemists*; Cambridge University Press: Cambridge, 1982. (b) Jennings, K. R.; Dolnikowski, G. G. *Methods in Enzymology*; McCloskey, J. A., Ed.; Academic Press: New York, 1990; p 37 and references therein.

10/1) to afford the product **9** as a yellowish solid. Yield 33 mg, 16  $\mu\text{mol}$  (40%). Mp 205–208 °C;  $^1\text{H NMR}$  ( $\text{CD}_2\text{Cl}_2$ , 295 K):  $\delta$  12.44 (s, 1 H), 9.84 (s, 1 H), 9.80 (s, 1 H), 9.49 (s, 1 H), 9.07 (s, 1 H), 8.97 (s, 1 H), 8.90–8.76 (2  $\times$  s, 2 H), 8.3 (apparent d + s, 2 H), 7.9–7.6 (m, 8 H), 7.55–7.05 (m, 12 H), 5.85–5.60 (4 mx t,  $J = 8$  Hz, 4 H), 2.8–0.5 (m, 122 H); ESI MS  $m/z$  2046 ( $[\text{M} + \text{H}]^+$ , calcd for  $\text{C}_{127}\text{H}_{156}\text{N}_{10}\text{O}_{14}$  2046).

**Metallocavitand 6.** A solution of cavitand **9** (13 mg, 6.6  $\mu\text{mol}$ ) and  $\text{ZnCl}_2$  (0.86 mg, 6.4  $\mu\text{mol}$ ) in 5 mL of  $\text{CHCl}_3/\text{MeOH}$  (4/1) was refluxed for 8 h. The solvent was removed under reduced pressure, and product **6** was obtained as a yellowish solid (14 mg, 100%). Mp 340–345 °C;  $^1\text{H NMR}$  ( $\text{CD}_2\text{Cl}_2$ , 295 K):  $\delta$  12.70 (s, 1 H), 9.84 (s, 1 H), 9.60 (s, 1 H), 9.32 (s, 1 H), 9.29 (s, 1 H), 9.08 (s, 2 H), 8.87 (s, 1 H), 8.66 (s, 1 H), 8.57 (d,  $J = 8.0$  Hz, 1 H), 8.1–7.0 (m, 20 H), 5.9–5.8 (m, 3 H), 5.68 (t,  $J = 8$  Hz, 1 H), 2.8–0.5 (m, 122 H); ESI MS  $m/z$  2178 ( $[\text{M} - \text{H}]^-$ , calcd for  $\text{C}_{127}\text{H}_{156}\text{Cl}_2\text{N}_{10}\text{O}_{14}\text{Zn}-\text{H}$  2178).

**Zn Complex 10.** Under  $\text{N}_2$  a solution of aldehyde **7**<sup>10</sup> (104 mg, 0.5 mmol) and 1,2-phenylenediamine (54 mg, 0.5 mmol) in nitrobenzene (8 mL) was stirred at 140 °C for 18 h. The solvent was evaporated under reduced pressure. The residue was purified by column chromatography ( $\text{CH}_2\text{Cl}_2$ ) to give the corresponding, metal-free **10** as a white solid (0.11 g, 75%). Mp 270–272 °C;  $^1\text{H NMR}$  ( $\text{CDCl}_3$ , 600 MHz, 295 K)  $\delta$  14.20 (br s, 1 H), 9.13 (dd,  $J = 3.7, 1.3$  Hz, 1 H), 8.73 (d,  $J = 8.3$  Hz, 1 H), 8.61 (d,  $J = 8.3$  Hz, 1 H), 8.55 (dd,  $J = 8.2, 1.5$  Hz, 1 H), 8.04 (m, 2H), 7.83 (dd,  $J = 8.2, 4.2$  Hz, 1 H), 7.78 (br, 1 H), 7.61 (br, 1 H), 7.27 (s, 2 H),  $^{13}\text{C NMR}$  ( $\text{CDCl}_3$ , 150.9 MHz, 295 K)  $\delta$  205.7, 149.9, 148.8, 146.6, 145.8, 137.6, 137.5, 127.4, 127.1, 124.1, 121.3; FTIR (KBr,  $\text{cm}^{-1}$ )  $\nu$  3062, 1619, 1589, 1436, 1316, 1277, 1082, 853; HR MALDI FTMS  $m/z$  297.1128 ( $[\text{M} + \text{H}]^+$ , calcd for  $\text{C}_{19}\text{H}_{12}\text{N}_4\text{H}$  297.1135).

1,10-Phenanthroline-2-carbaldehyde **7** was synthesized using a reliable literature procedure,<sup>10</sup> but instead, of the reported  $\text{SeO}_2$  oxidation,

a Dess–Martin reaction was employed, which was slower (14 h) but gave almost quantitative yield. All of the analytical and spectral data were identical to that reported.<sup>16b</sup> Under  $\text{N}_2$  to a solution of 1,10-phenanthroline-2-carbinol (0.36 g, 1.7 mmol) in  $\text{CH}_2\text{Cl}_2$  (50 mL) was added Dess–Martin reagent (commercial, (1,1,1-triacetoxy)-1,1-dihydro-1,2-benziodoxol-3(1H)-one) (1.78 g, 4.2 mmol). The resulting mixture was stirred at 55 °C for 8 h, giving a clear solution. The solution was cooled to room temperature, and water (30 mL) was added. After separation, the aqueous layer was extracted with  $\text{CHCl}_3$  (30 mL) twice. The combined solution was dried over  $\text{Na}_2\text{SO}_4$  and evaporated to yield **7** as a white solid (0.32 g, 90%), which was pure enough for next step.

Under Ar, to a solution of metal-free **10** (8 mg, 0.027 mmol) in  $\text{CHCl}_3/\text{MeOH}$  (1/1, 5 mL) was added a THF solution of  $\text{ZnCl}_2$  (54  $\mu\text{L}$ , 0.027 mmol) dropwise. The resulting mixture was refluxed for 8 h. The solvent was removed under reduced pressure, and zinc complex **10** was obtained as a yellowish solid (8.0 mg, 73%). Mp >350 °C;  $^1\text{H NMR}$  ( $\text{DMSO}-d_6$ , 600 MHz, 295 K)  $\delta$  14.62 (br s, 1 H), 9.17 (apparent s, 2 H), 8.84 (apparent s, 1 H), 8.81 (apparent s, 1 H), 8.32 (apparent s, 2 H), 8.16 (apparent s, 1 H), 7.94 (apparent s, 1H), 7.84 (apparent s, 1 H), 7.50 (apparent s, 2 H); FTIR (KBr,  $\text{cm}^{-1}$ )  $\nu$  3448, 1589, 1512, 1448, 1321, 983, 856; HR MALDI FTMS  $m/z$  395.0037 ( $[\text{M} - \text{Cl}]^+$ , calcd for  $\text{C}_{19}\text{H}_{12}\text{N}_4\text{ClZn}$  395.0036).

**Acknowledgment.** We are grateful for financial support from the Skaggs Research Foundation and the National Institutes of Health. U.L. thanks Alexander von Humboldt Stiftung, Feodor-Lynen program for the scholarship. J.C. is a Skaggs Postdoctoral Fellow.

JA011488M